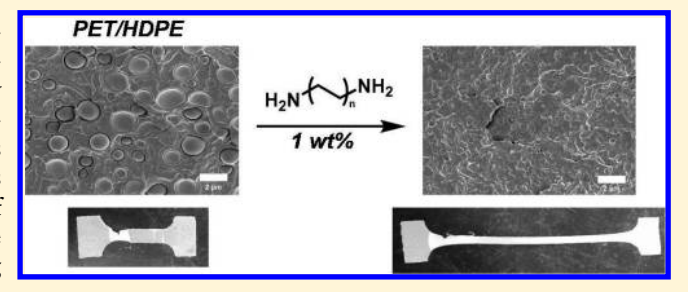
Macromolecules

Reactive Compatibilization of Poly(ethylene terephthalate) and High-Density Polyethylene Using Amino-Telechelic Polyethylene

Alexander D. Todd,[†] Ryan J. McEneany,[§] Vasily A. Topolkaraev,[§] Christopher W. Macosko,[‡] and Marc A. Hillmyer*, †

Supporting Information

ABSTRACT: Low molar mass (3-17 kg/mol) amino-telechelic polyethylene (ATPE) was used to reactively compatibilize poly(ethylene terephthalate) (PET) and high-density polyethylene (HDPE) via ester aminolysis of PET. A tertbutyloxycarbonyl (Boc)-protected polyethylene precursor was thermolytically deprotected during the melt-blending process to render the reactive amine termini. Spectroscopic analysis of a model reaction confirmed the presence of amide functionality in the resultant material. Through blending studies, we found that low loadings of ATPE (0.5 wt %)



significantly reduced the volume of the dispersed HDPE phase particles by a factor of 8 when compared to a binary PET/HDPE blend as assessed by scanning electron microscopy (SEM). Mechanical analysis of the ATPE-compatibilized blends showed a 12fold increase in the elongation at break over the unmodified PET/HDPE blend. Ultimately, the results here offer a new approach to reactively compatibilize and toughen PET/HDPE blends and open the door for other uses of amino-telechelic polyethylene.

INTRODUCTION

Reactive compatibilization has been an effective longstanding tool to compatibilize immiscible polymer blends. 1,2 At the heart of reactive compatibilization is a functionalized polymeric additive that can undergo a chemical transformation with either the matrix polymer phase or the dispersed polymer phase under normal blending conditions. For example, a compatibilizer may be miscible or partially miscible with the dispersed phase of the blend and, however, be only reactive toward the matrix polymer. Ultimately, a hybrid graft or block polymer is formed during processing that has the ability to reduce the droplet size of the dispersed phase as well as promote adhesion between the dispersed and matrix phases.

The most common reactive functionalities include epoxide and maleic anhydride derivatives that are prone to ring-opening reactions in the presence of a nucleophilic end or pendant group (e.g., hydroxyl group). The most common epoxyfunctionalized compatibilizers are copolymers of ethylene and glycidyl methacrylate (PEGMA) or terpolymers of ethylene, methyl acrylate, and glycidyl methacrylate (PEGMMA). Conversely, maleic anhydride is often incorporated through a postpolymerization free-radical grafting reaction to polyolefins (POs). Both compatibilizers have shown to be useful for a variety of blends with differing compositions including polyamide/linear low-density polyethylene (LLDPE),3 poly-(butylene terephthalate) (PBT)/polycarbonate (PC), poly-(lactic acid) (PLA)/polypropylene (PP), poly(ethylene

terephthalate) (PET)/high-density polyethylene (HDPE),6 and PET/LLDPE.

Blends based on commodity plastics such as PET and POs are particularly intriguing in regards to the upside of developing high-performance materials at relatively low cost. Moreover, blending recycled PET and HDPE represents an effective way to better utilize waste materials. As such, there have been multiple disclosures of compatibilizing PET/PO blends using epoxy and maleic anhydride functionalized polymers. In general, the addition of a glycidyl or maleic anhydride functionalized polymer leads to reduced droplet size of the dispersed phase and improved mechanical properties of the resulting PET/PO blends. 5,6

Inspired by previous studies regarding ethylenediamine aminolysis of PET and in efforts to expand the scope of reactive compatibilization for PET/HDPE blends, we envisioned that amino-telechelic polyethylene (ATPE) could react with the ester linkages of PET, affording a PET-PE multiblock poly(ester amide) that would ultimately serve as a blend compatibilizer (Scheme 1).8-11 Compatibilization via aminolvsis is advantageous in that the reaction proceeds without catalysis and has been previously demonstrated in PET/polyamide and polycarbonate/polyamide blends. 12-15 Furthermore, ATPE can cocrystallize with the HDPE phase, potentially

September 23, 2016 Received: Revised: November 15, 2016 Published: November 29, 2016

Department of Chemistry and Department of Chemical Engineering and Materials Science, University of Minnesota, Minneapolis, Minnesota 55455, United States

[§]Corporate Research and Engineering, Kimberly-Clark Corporation, Neenah, Wisconsin 54956, United States

Scheme 1. Proposed Reaction of ATPE with PET To Form a PET-PE Multiblock Polymer Compatibilizer

leading to enhanced compatibilization compared to amorphous compatibilizers such as PEGMA and PEGMMA.

ATPE can be accessed by ring-opening metathesis polymerization (ROMP) of cyclooctene (COE) with an appropriate chain transfer agent (CTA) to install the reactive chain termini. Moreover, ROMP offers synthetic versatility with respect to generating various PO structures with the ease of alkylation of COE at the 3-position relative to the olefin. Here, we demonstrate that low loadings (0.5 wt %) of ATPE can reactively compatibilize PET/HDPE blends and dramatically reduce the dispersed phase volume. Overall, the mechanical properties of the blends containing the ATPE compatibilizer exhibit significantly enhanced toughness compared to the unmodified PET/HDPE blend.

■ EXPERIMENTAL SECTION

General. All manipulations were carried out in oven- or flame-dried glassware under a positive pressure of Ar or in a N_2 filled MBraun glovebox unless otherwise noted. Reagents and solvents were purchased from commercial sources. CHCl $_3$ was vacuum transferred from CaH $_2$ and then stored over molecular sieves (3 Å). Cyclooctene (COE) from Acros Organics was distilled from CaH $_2$ and stored at $-20~^{\circ}$ C. Di-tert-butyl but-2-ene-1,4-diyl(E)-dicarbamate (Boc $_2$ CTA) 19 and (E)-2,2'-(but-2-ene-1,4-diyl)bis (isoin doline-1,3-dione) (Phth $_2$ CTA) 20 were synthesized by modified published procedures. PET was purchased from Indorama (PET 8902, [η] = 0.85 dL/g in dichloroacetic acid as indicated from Indorama). The M_n of the PET was estimated to be 25 kg/mol by the Mark—Houwink equation using the reported intrinsic viscosity and $K=49\times10^{-4}$ and $\alpha=0.49$ in dichloroacetic acid. 21 HDPE was provided by the Dow Chemical Company (DMDA 8904, $M_{w,SEC}=144~{\rm kg/mol}$, D=4.40).

Molecular Characterization. ¹H NMR spectra were recorded on a Bruker Avance III HD 400 MHz spectrometer. Chemical shifts (δ) are reported in parts per million (ppm) downfield from tetramethylsilane (TMS) at 0.0 ppm and referenced to residual protio solvent (CDCl₃ = 7.24 ppm, PhMe- d_8 = 2.08 ppm). Coupling constants (J) are expressed in hertz (Hz). Size exclusion chromatography (SEC) measurements were collected on a Hewlett-Packard 1100 series pump and a Hewlett-Packard 1047A refractive index detector. Three PLgel columns (Polymer Laboratories columns with 500, 103, and 104 Å pore sizes) were used in series and maintained at 35 °C. CHCl₃ was the mobile phase, and numberaverage molar mass (M_n) and molar mass distributions (D) are referenced to polystyrene standards. High-temperature SEC measurements were collected on a PL-GPC 220 (Agilent Systems) system using 1,2,4-trichlorobenzene as the eluent referenced to polystyrene standards at 135 °C. Fourier-transform infrared (FTIR) spectra were collected on a Bruker Alpha-P Platinum spectrometer equipped with a platinum attenuated total reflectance (ATR) attachment (diamond crystal). Intrinsic viscosities were measured with an Ubbelohde Type OC D125 tube in dichloroacetic acid at 35 °C. Blends containing HDPE or ATPE were filtered through a 0.2 µm PTFE syringe filter prior to analysis. A concentration of 3 mg/mL was used, and the intrinsic viscosity was estimated using the Billmeyer equation.

Thermal Analysis. Thermogravimetric analyses were conducted on a TA Instruments TGA500. Samples were heated under nitrogen at a ramp rate of 10 °C/min to 550 °C. Differential scanning calorimetry

(DSC) measurements were performed on a TA Instruments Q1000 Discovery Series with a heating rate of 5 $^{\circ}$ C/min.

Preparation of Blends and Sample Preparation. Blends were prepared on an Xplore MC 5 microcompounder. Prior to blending, all polymers were dried under vacuum at 100 °C for a minimum of 18 h. Blends were compounded at 50 rpm for 10 min at 265 °C, then extruded and allowed to cool to ambient temperature, and dried at 100 °C prior to further processing. Compression-molded tensile specimens (22 mm × 5 mm × 0.5 mm) were prepared on a hydraulic hot press with a plate temperature of 270 °C. Samples were kept on the bottom plate for 3 min and then compressed at 14 MPa for 2 min. The mold was subsequently cooled on a cold water-jacketed press where the mold was held for 10 min.

Mechanical Testing. Tensile specimens were allowed to age for 24 h at ambient temperature prior to mechanical analysis. Tensile tests were performed on an Instron Model 1011 following ASTM D1708 standard. Test conditions: load range = 1000 N; rate = 5 mm/min. Mechanical data were averaged over five runs.

Microscopy. Scanning electron microscopy (SEM) was conducted on a Hitachi S4700 microscope. Samples were placed in a liquid N_2 bath for approximately 15 min. The samples were removed and quickly fractured with a razor blade and then mounted on double-sided carbon tape. All blends were sputter-coated with 5 nm of Pt before SEM analysis. The diameter of the dispersed HDPE phase was calculated using ImageJ software counting 100 particles.

Representative ROMP Procedure for Boc-ATPCOE. A flamedried Schlenk flask equipped with a stir bar was charged with Boc₂CTA (88 mg, 0.31 mmol), COE (2.0 mL, 15.35 mmol), and CHCl₃ (4.0 mL). After dissolution, the solution was subjected to three successive freeze-pump-thaw cycles. The flask was then placed under a positive pressure of Ar and placed in a 40 °C oil bath. In the glovebox, SIMesRuCHPh(PCy₃)Cl₂ (3 mg, 3.5 μ mol) was dissolved in CHCl₃ (0.5 mL) and drawn into a 1.0 mL syringe. The needle of the syringe was capped with a rubber septum, removed from the glovebox, and then injected into the aforementioned flask containing the CTA, monomer, and solvent. The resulting mixture became viscous within 15 min and was allowed to stir for 18 h. Upon completion, ethyl vinyl ether (0.1 mL) was added to flask to terminate the polymerization. The mixture was diluted with CHCl₃, and the Boc-protected aminotelechelic poly(cyclooctene) (Boc-ATPCOE) was precipitated in MeOH (200 mL). The polymer was isolated and dissolved in CHCl₃ and reprecipitated into MeOH (200 mL). The process of dissolution and precipitation was repeated for an additional cycle. The resulting material was then dried under reduced pressure at 50 °C for 24 h and isolated as an off-white solid (1.44 g, 81%). $M_{n.NMR} = 6.0 \text{ kg/}$ mol, $M_{\rm n,SEC} = 14.8 \text{ kg/mol}$, D = 2.14. ¹H NMR (400 MHz, CDCl₃): δ 5.36 (t, trans CH=CH, J = 3.5 Hz), 5.32 (t, cis CH=CH, J = 5 Hz), 1.95 (m, CH=CH- CH_2 -), 1.43 (s, tBu), 1.28 (m, $-CH_2$ -). Boc-ATPCOE-3: $M_{\rm n,NMR}=3.0~{\rm kg/mol},~M_{\rm n,SEC}=6.8~{\rm kg/mol},~D=1.56.$ Boc-ATPCOE-17: $M_{\rm n,NMR}=17.0~{\rm kg/mol},~M_{\rm n,SEC}=52.0~{\rm kg/mol},~D=1.56.$

Representative Chemical Hydrogenation Procedure. A round-bottom flask equipped with a stir bar was charged with Boc-ATPCOE (1.00 g, 9.07 mmol of repeat unit) and BHT (1 crystal, ca. 2–5 mg). The solids were dissolved in xylenes (120 mL) upon which TsNHNH₂ (3.39 g, 18.20 mmol), and *n*-Bu₃N (4.6 mL, 19.31 mmol) was added. The flask was fitted with a reflux condenser, and the resulting solution was then heated to reflux for 18 h. After cooling to ambient temperature, the mixture was poured into MeOH (100 mL). The hydrogenated polymer was washed successively with copious

amounts of MeOH and acetone. The material was then dried under vacuum at 50 °C for 24 h and isolated as a light yellow solid (0.99 g, 98%). $M_{\rm n,NMR}=6.0~{\rm kg/mol},~M_{\rm n,SEC}=7.8~{\rm kg/mol},~D=2.33.~{\rm ^{1}H}~{\rm NMR}$ (400 MHz, PhMe- $d_{\rm g}$): δ 2.93 (q, BocHN– $CH_{\rm 2}$ –, $J=8~{\rm Hz}$), 1.42 (s, 'Bu), 1.33 (s, –CH₂–). Boc-ATPE-3: $M_{\rm n,NMR}=3.3~{\rm kg/mol},~M_{\rm n,SEC}=3.2~{\rm kg/mol},~D=2.25.~{\rm Boc-ATPE-17}:~M_{\rm n,NMR}=17.0~{\rm kg/mol},~M_{\rm n,SEC}=28.5~{\rm kg/mol},~D=2.06.$

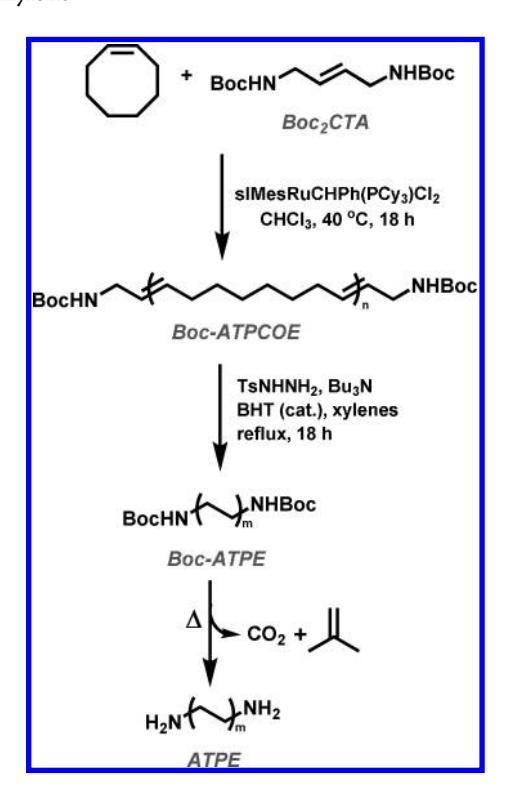
Representative Blending Procedure. Dried PET (4.005 g), HDPE (0.450 g), and Boc-ATPE-6 (45 mg) were added to a preweighed vial and manually mixed. The temperature setting on the microcompounder was adjusted to 265 °C for all three zones, and the mixing speed was set to 50 rpm. The polymer was introduced to the mixer using the hopper attachment. Mixing was allowed to occur for 10 min under a N_2 purge, and then the blend was extruded onto a glass plate and allowed to cool to ambient temperature. The extruded polymer was then manually cut into smaller pieces for further analyses and compounding.

■ RESULTS AND DISCUSSION

Amines are known to poison Ru-based metathesis catalysts; thus, a suitable protecting group was installed on the CTA. We chose the acid labile *tert*-butyloxycarbonyl (Boc) group due to the high temperature thermolytic cleavage giving isobutylene and CO₂. In polymeric systems, Wagener and co-workers demonstrated that pendant Boc-protected amino groups in ethylene—vinylamine copolymers underwent thermolysis around 220 °C. Verall, thermal deprotection presents a unique opportunity in terms of reactive compatibilization. Considering blending parameters for PET, which has a melting transition of approximately 260 °C, the Boc-protected precursor could be used directly and deprotection would take place during blending, effectively eliminating a separate deprotection step.

Boc-protected amino CTAs have been successfully employed in the ROMP of cyclooctadiene, and Scheme 2 shows the

Scheme 2. Synthesis of Boc-Protected Amino-Telechelic Polyethylene



synthetic strategy employed to access ATPE. ¹⁶ The ROMP of COE in the presence of di-tert-butyl but-2-ene-1,4-diyl(E)-dicarbamate (Boc₂CTA) using SIMesRuCHPh(PCy₃)Cl₂ (Grubbs second-generation catalyst) afforded Boc-protected amino telechelic poly(cyclooctene) (Boc-ATPCOE). ¹H NMR spectroscopic analysis of Boc-ATPCOE revealed the expected olefin and methylene resonances as well as a singlet at 1.43 ppm in CDCl₃ corresponding to the ^tBu on the termini of the polymer. The polymerization was amenable to various molar masses (3–17 kg/mol) as determined by ¹H NMR spectroscopy end-group analysis (assuming exactly two end groups per chain).

The Boc-ATPCOE was chemically hydrogenated using *p*-tosyl hydrazide to afford Boc-protected ATPE (Boc-ATPE).

Table 1. Molecular Characterization of ATPE Samples

material	${M_{ m n,NMR}}^a ({ m kg/mol})$	${M_{ m n,SEC}}^{b} \ m (kg/mol)$	Ð	yield ^c (%)	
Boc-ATPE-3	3.3	3.2	2.25	79	
Boc-ATPE-6	6.0	7.8	2.33	>99	
Boc-ATPE-17	17.0	28.5	2.06	>99	

 $^{a1}{\rm H}$ NMR spectrum conducted in PhMe- d_8 at 100 °C, $^{\rm t}{\rm Bu}$ singlet referenced to 18. $^{\rm b}{\rm SEC}$ measured using 1,2,4-trichlorobenzene at 135 °C referenced to polystyrene standards. $^{\rm c}{\rm Isolated}.$

Molecular characterization data are summarized in Table 1. The 1 H NMR spectrum for the Boc-ATPE showed resonances corresponding to the methylene repeat unit of the PE backbone at 1.33 ppm, the methylenes alpha to the nitrogen end groups at 2.93 ppm, and a singlet at 1.42 ppm for the methyl groups on the Boc group in toluene- d_8 at 100 $^{\circ}$ C. Furthermore, the molar masses of the ATPE derivatives, assessed by 1 H NMR spectroscopy, were consistent with the PCOE precursors (assuming exactly two end groups per chain).

Thermogravimetric analysis (TGA) was used to analyze mass loss as a function of temperature. Figure 1 shows the TGA

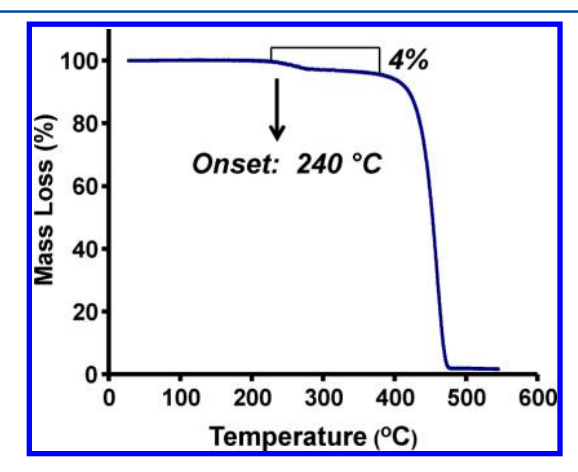


Figure 1. TGA curve of Boc-protected ATPE-6 at 10 °C/min.

curve for the Boc-ATPE-6 material. Mass loss begins at 240 $^{\circ}$ C at a 10 $^{\circ}$ C/min heating rate and then stabilizes until rapid decrease at 425 $^{\circ}$ C. The theoretical mass loss of isobutylene and CO₂ for 6 kg/mol ATPE is 3.3%, which is in agreement with the experimentally observed 4%. Furthermore, isothermal experiments at 265 $^{\circ}$ C show that after 10 min mass loss was 3% (90% deprotection based on the theoretical value), which is

conducive for melt-blending (Figure S11). Fourier-transform infrared spectroscopy (FTIR) was used to monitor the carbamate stretching frequency pre- and postheating. Figure S12 shows the spectral overlay of Boc-ATPE-6 before heating and after subjection to 275 °C under dynamic vacuum for 10 min. After thermal treatment, the carbamate stretching frequency at 1710 cm⁻¹ is no longer evident, suggestive of deprotection. Thermolysis of the Boc group was also confirmed by high-temperature ¹H NMR spectroscopy in toluene-d₈; the absence of the ^tBu singlet at 1.42 ppm for the thermally treated material (please see Figure S13) is also consistent with deprotection. Also, the resonances of the methylenes alpha to the nitrogen shifted from 2.92 ppm for Boc-ATPE-6 to 2.52 ppm for ATPE-6. To confirm the presence of the terminal amine groups, the aforementioned thermally treated material was subjected to the ninhydrin test upon which a deep purple color ensued.²⁵ Taken together, the spectroscopic analysis and chemical test demonstrate that the thermal deproptection of Boc-ATPE occurs cleanly and the terminal amines are generated.

To examine the feasibility of the proposed aminolysis between PET and ATPE, model substrates were used to test the reaction (Scheme S1). Boc-ATPE-3 was mixed with low molar mass PET (~2 kg/mol, see Supporting Information) and then heated at 265 °C for 10 min under an atmosphere of argon. The resulting material was washed with 1,1,2,2tetrachloroethane (TCE) at 120 °C to remove any unreacted PET or Boc-ATPE/ATPE and subsequently analyzed by FTIR spectroscopy. Given that low molar mass PET is only sparingly soluble in TCE, we reasoned that the PET-rich regions of the proposed PE-PET poly(ester amide) will cause the material to be insoluble.²⁶ Figure 2 shows the FTIR spectral overlay of the corresponding polymeric product along with the starting materials. In addition to the vibrational stretches of both PET and HDPE, there is a band at 1658 cm⁻¹ indicative of an amide stretching frequency for the isolated material after the reaction (Figure 2d). The aforementioned band was not observed for any of the starting materials (Boc-ATPE-3 or PET) or intermediates (ATPE-3). Thus, the results from the model substrate test reactions suggested to us that indeed ATPE was reacting with PET to form a diblock or multiblock poly(ester amide) as described in Scheme 1.

Having established the thermolytic stability of the Boc end groups of Boc-ATPE and aminolysis of low molar mass PET, melt-blending studies were performed using a twin-screw microcompounder at 265 °C for 10 min. At the conclusion of mixing, the blends were extruded and allowed to cool to ambient temperature. Differential scanning calorimetry of the blends showed that ATPE had a minimal effect on the thermal properties of the matrix PET (summarized in Table S1). The $T_{\rm g}$ and $T_{\rm m}$ of the PET for all blends was approximately 79 and 252 °C, respectively. The percent crystallinity (χ_c) of the PET matrix was approximately 35% for all blends. Likewise, the $T_{\rm m}$ for the PE component, regardless of the presence of ATPE, was 128 °C for all blends. The χ_c of PE for the PET/HDPE and PET/HDPE/ATPE-3 blends was 60% but decreased to 40% for the ATPE-6 and ATPE-17 analogues. Solution state viscometric measurements of the PET matrix revealed that the ATPE had minimal effect on the molar mass of the PET (Table S2). The intrinsic viscosity of processed PET and the extracted PET from the ATPE-containing blends were both about 0.7 dL/g in dichloroacetic acid at 35 °C.

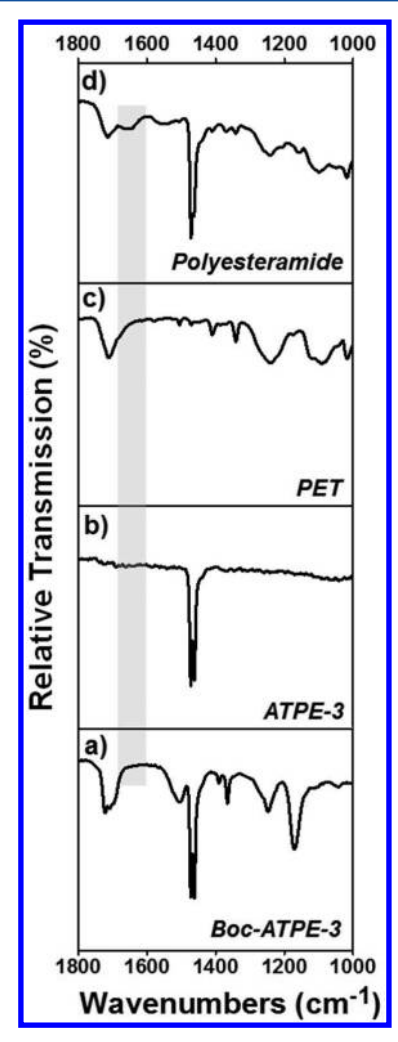


Figure 2. Spectral overlay of Boc-ATPE-3 (a), ATPE-3 (b), low molar mass PET (c), and the isolated material after the reaction of ATPE-3 and PET (d).

The morphology of the blends was subsequently assessed by scanning electron microscopy (SEM) of cryofractured surfaces prior to mechanical testing. Fracturing the samples at cryogenic temperatures was employed to prevent smearing of the PET or HDPE phases. Figure 3 depicts the SEM images of the blends after sputter-coating with 5 nm of Pt. The dispersed HDPE phase in the binary blend of PET/HDPE (90/10) showed an average diameter of 1.2 \pm 0.2 μ m, corresponding to a volume of approximately 0.91 μ m³. Examination of the interface of the binary PET/HDPE blend shows a noticeable gap between the two phases. This gap could be partially attributed to the incompatibility of PET and HDPE as well as thermal contraction of HDPE during the cooling portion of processing. Blends with ATPE-3, ATPE-6, or ATPE-17 at 1 wt % showed significant reduction in the diameter ($d = 0.5 \pm 0.1 \mu m$) of the dispersed phase (Figure 3b-d). Furthermore, examination of Figure 3e shows that blends containing lower loadings of ATPE-6 (0.5 wt %) also leads to a significant and comparable reduction in the diameter of the HDPE phase ($d = 0.6 \pm 0.1$ μ m). Overall, at 0.5 and 1 wt % ATPE loading, the volume of the dispersed HDPE phase particles is reduced by a factor of 8 and 14, respectively. Moreover, the surface area to volume ratio for the HDPE phase in the compatibilized blends is higher than the uncompatibilized blend by a factor of 2. The reduction in

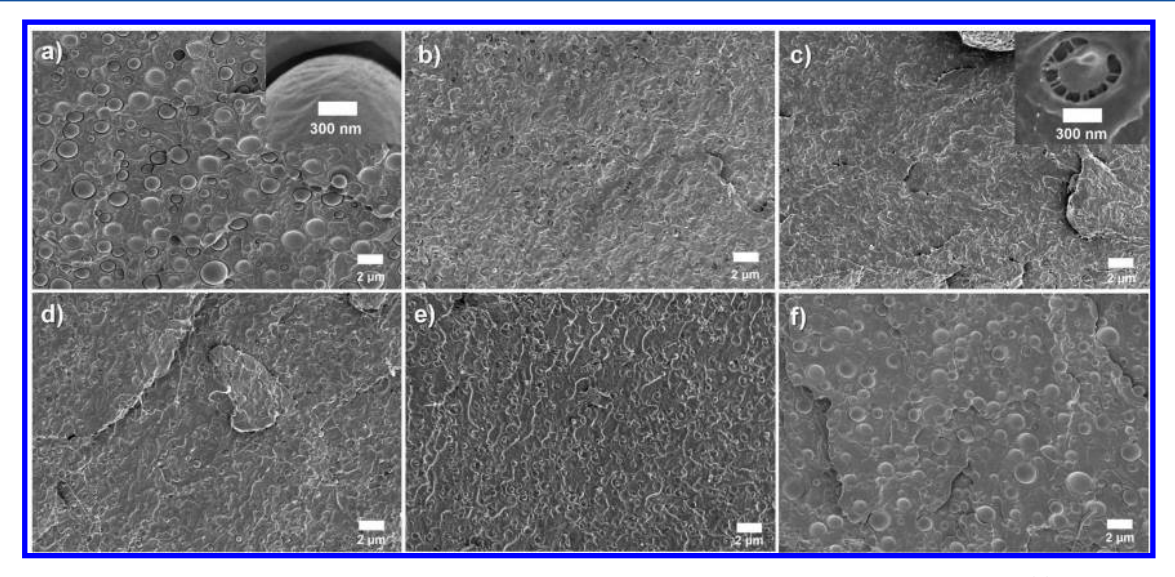


Figure 3. SEM images of blends. All blends were cryofractured at -196 °C and coated with 5 nm of Pt prior to analysis. (a) PET/HDPE (90/10); (b) PET/HDPE/ATPE-3 (89/10/1); (c) PET/HDPE/ATPE-6 (89/10/1), inset: higher magnification of fibrillar structure at PET/HDPE interface; (d) PET/HDPE/ATPE-17 (89/10/1); (e) PET/HDPE/ATPE-6 (89.5/10/0.5), (f) PET/HDPE/HDPE-4 (89/10/1). Scale bar = 2 μm. For higher magnification images, see Figures \$18-\$28.

Table 2. Mechanical Properties^a

material	composition	E^{b} (GPa)	$\sigma_{\mathrm{YS}}^{}}}}}}$ (MPa)	$\sigma_{\mathtt{P}}^{}d}$ (MPa)	$\varepsilon_{\mathrm{b}}^{e}$ (%)	toughness (MJ/m³)
PET	100	2.0 ± 0.1	52 ± 3	33 ± 2	261 ± 29	93 ± 15
PET/HDPE	90/10	1.9 ± 0.1	48 ± 2	32 ± 3	15 ± 2	3 ± 1
PET/HDPE/ATPE-3	89/10/1	1.9 ± 0.0	46 ± 2	30 ± 2	243 ± 45	79 ± 17
PET/HDPE/ATPE-6	89/10/1	1.8 ± 0.2	47 ± 2	31 ± 2	271 ± 30	92 ± 13
PET/HDPE/ATPE-17	89/10/1	1.9 ± 0.1	48 ± 1	32 ± 2	219 ± 35	74 ± 15
PET/HDPE/ATPE-6	89.5/10/0.5	2.0 ± 0.1	46 ± 1	30 ± 2	237 ± 16	72 ± 8
PET/HDPE/HDPE-4	89/10/1	1.9 ± 0.1	48 ± 4	32 ± 4	28 ± 18	8 ± 6

^aTensile tests conducted on an Instron Model 1011. Load range = 1000 N; rate = 5 mm/min. ^bElastic modulus; measured from the linear portion of the stress–strain curve (initial 1%). ^cYield stress. ^dPlateau stress. ^eElongation at break.

volume and surface area to volume ratio of the HDPE particles demonstrates the efficacy of the proposed PET–PE multiblock poly(ester amide) formed during blending to reduce the interfacial tension between the two phases. The number of PE blocks (from ATPE) per surface area of dispersed phase also gives an indication of compatibilization efficacy. Thus, on the basis of the theoretical volume of HDPE in the blends, we estimate that the number of PE blocks/nm² for the blends range from 0.3 to 1. The highest PE block content arises from the 1 wt % ATPE-3 (1 PE block/nm²) containing blend and the lowest from the 1 wt % ATPE-17 (0.3 PE blocks/nm²) blend.

Close inspection of the interface between the matrix and dispersed phase at higher magnification of the ATPE-containing blends show a fibrillar structure that spans the void between two phases (inset in Figure 3c and Figures S21, S23, S25). In contrast, these fibrils were not observed for the binary PET/HDPE blend (inset in Figure 3a). The presence of the fibrils in the ATPE-containing blends was suggestive of an increased level of adhesion between the PET and HDPE. Similar fibril-like structures have been observed in PET/HDPE/PEGMA²⁷ and PLA/HDPE blends compatibilized with PLA-PE block polymers (PLA-b-PE).²⁸ In the former, the fibrils were attributed to HDPE deformation without dislodgement from the PET matrix during the cryofracture process. For the latter, the fibrils were observed in the fracture surfaces of impact specimens of blends compatibilized with PLA-b-PE

whereas the fibrils were absent in uncompatibilized blends. Considering the PET/HDPE/ATPE blends were cryofractured prior to SEM analysis, we assume that sufficient force was generated to cause deformation to the HDPE phase which gives rise to the fibrillar structure at the PET/HDPE interface due to chain entanglement and crystallization with the PET-PE multiblock poly(ester amide) compatibilizer.

A control experiment was conducted to determine whether the difference in morphology of the ATPE-containing blends was due to a low molar mass phenomenon rather than what we suggest is PET-PE poly(ester amide) formed from the aminolysis of PET by ATPE. Thus, a 4.0 kg/mol methylterminated (i.e., unfunctionalized) HDPE derivative (HDPE-4) was synthesized in a similar manner as the Boc-ATPE. An analogous blend was prepared of PET/HDPE/HDPE-4 (89/ 10/1 wt %) and analyzed using SEM (image shown in Figure 3f). From the SEM image, the overall morphology of the PET/ HDPE/HDPE-4 blend is very similar to the PET/HDPE (90/ 10) blend with the dispersed phase having an average diameter of 1.1 \pm 0.4 μ m. Moreover, as with the binary PET/HDPE blend, the PET/HDPE/HDPE-4 blend did not exhibit the fibrillar structure at the interface as in the ATPE-containing blends. As such, we concluded from the SEM analysis of the control blend that the compatibilization of PET and HDPE was a result of the ATPE rather than incorporation of a low molar mass additive.

To further demonstrate the necessity of a thermally labile nitrogen protecting group, an additional control blend was prepared with phthalimido-telechelic polyethylene (Phth-PE), a more thermolytically stable protecting group compared to Boc. Using a similar strategy to the Boc-ATPE materials, Phth-PE $(M_n = 6.7 \text{ kg/mol}, D = 2.75)$ was synthesized, and its thermolytic stability was established via TGA (Supporting Information). Inspection of the TGA curve (Figure S16) shows that Phth-PE possesses an onset mass loss temperature of 396 °C under a nitrogen atmosphere at a heating rate of 10 °C/min. Isothermal analysis of Phth-PE at 265 °C shows approximately 0.5% mass loss (11% deprotection based on theoretical value) over a 10 min period (Figure S17). Thus, Phth-PE was determined to be relatively stable under the same processing conditions for the Boc-ATPE blends. A blend of PET/HDPE/ Phth-ATPE (89/10/1) was prepared in analogous manner, and the morphology was examined using SEM (Figures S30-S32). Upon addition of 1 wt % Ph-ATPE, the dispersed PO phase had an average diameter size of 1.6 \pm 0.7 μ m-220% higher than the ATPE-containing analogues. Similar to the PET/ HDPE and PET/HDPE/HDPE-4 blends, the PET/HDPE/ Phth-PE blend did not possess the fibrillar structure at the interface between PET and PO phases (Figure S32). The SEM analysis demonstrated that Phth-PE was ineffective at compatibilizing PET and HDPE, and the amine termini in ATPE are critical for compatibilization.

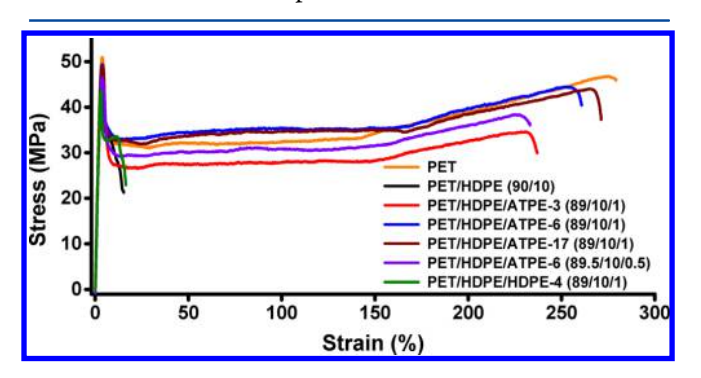


Figure 4. Representative stress—strain curves for PET/HDPE and PET/HDPE/ATPE blends.

The effect of the ATPE reactive compatibilizer on the mechanical properties of the blends was investigated by uniaxial tensile tests of compression-molded specimens. Table 2 summarizes the key results of the aforementioned experiments, and representative stress-strain curves are shown in Figure 4. The elastic moduli (E), yield stress (σ_{YS}), and plateau stress $(\sigma_{\rm p})$ for all the materials were similar (~1.9 GPa, ~50 MPa, and ~30 MPa, respectively), regardless of the ATPE loading or molar mass of the ATPE additive, which can be partially attributed to relatively low sensitivity of bulk properties such as elastic moduli and yield stress to 10% mass loading of HDPE in the blends. On the other hand, the elongation at break $(\varepsilon_{\rm b})$ for the binary PET/HDPE blend was relatively poor with an average of 15%. Upon incorporation of the ATPE compatibilizer, a significant increase (~12-fold) in the $\varepsilon_{\rm b}$ for the blends was observed for all molar masses and loadings of the ATPE compatibilizer, approaching $\varepsilon_{\rm b}$ values similar to that of the unmodified PET homopolymer. We attribute the increase in ductility to a reduced size of secondary phase inclusions, improved adhesion between the PET and HDPE phases from the compatibilization by the PET-PE multiblock poly(ester

amide), and more efficient stress transfer to the ductile HDPE phase. For the uncompatibilized blend, premature fracture could arise from the debonding of the PET/HDPE phases due to poor adhesion and the larger-sized inclusions. The control blend, PET/HDPE/HDPE-4, exhibited similar mechanical properties to the binary blend with an average $\varepsilon_{\rm b}$ of 28%. Collectively, the addition of the ATPE compatibilizer significantly toughened the PET/HDPE blends at low loadings.

CONCLUSION

We have shown that amino-telechelic PE can be used as a reactive compatibilizer for PET/HDPE blends at low loadings (0.5 wt %) via an aminolysis reaction with PET. Thermogravimetric and spectroscopic analysis demonstrated that the Bocprotected ATPE undergoes thermal deprotection during the blending process to render reactive amine termini. SEM analysis of the aforementioned blends revealed an 8-fold and 14-fold reduction in dispersed phase particle volume upon addition of 0.5 and 1 wt % ATPE, respectively. All molar masses of ATPE were able to reduce the volume of the dispersed HDPE phase upon incorporation into a binary blend of PET/HDPE. Uniaxial extension experiments revealed that the ATPE compatibilizer did not significantly reduce the elastic modulus or yield stress of the PET matrix. Conversely, the ATPE-containing blends had significantly higher elongation at break values that were within error of the PET homopolymer and up to a 12-fold increase relative to the binary blend. Overall, the results presented here serve as a platform for using ATPE as a reactive compatibilizer for toughening high-melting polyester/polyolefin blends.

ASSOCIATED CONTENT

S Supporting Information

The Supporting Information is available free of charge on the ACS Publications website at DOI: 10.1021/acs.macromol.6b02080.

Further experimental details, spectra, SEM images, and thermal data (PDF)

AUTHOR INFORMATION

Corresponding Author

*E-mail: hillmyer@umn.edu (M.A.H.).

ORCID 6

Alexander D. Todd: 0000-0002-8330-2586 Marc A. Hillmyer: 0000-0001-8255-3853

Notes

The authors declare no competing financial interest.

ACKNOWLEDGMENTS

We graciously thank the Kimberly Clark Corporation for their financial support of this project. Partial support was provided by the NSF under the Center for Sustainable Polymers, CHE-1413862. Parts of this work were carried out in the Characterization Facility, University of Minnesota, a member of the NSF-funded Materials Research Facilities Network via the MRSEC program.

REFERENCES

(1) Xanthos, M.; Dagli, S. S. Compatibilitation of Polymer Blends by Reactive Processing. *Polym. Eng. Sci.* **1991**, *31*, 929–935.

(2) Passaglia, E.; Coiai, S.; Augier, S. Control of macromolecular architecture during the reactive functionalization in the melt of olefin polymers. *Prog. Polym. Sci.* **2009**, *34*, 911–947.

- (3) Padwa, A. R. Compatibilized blends of polyamide 6 and polyethylene. *Polym. Eng. Sci.* **1992**, *32*, 1703–1710.
- (4) He, J.; Guo, Y.; Sun, S.; Zhang, H. Influence of methyl methacrylate-co-glycidyl methacrylate copolymers on the compatibility, morphology and mechanical properties of poly(butylene terephthalate) and polycarbonate blends. *J. Polym. Eng.* **2015**, 35, 247–256.
- (5) Xu, Y.; Loi, J.; Delgado, P.; Topolkaraev, V.; McEneany, R. J.; Macosko, C. W.; Hillmyer, M. A. Reactive Compatibilization of Polylactide/Polypropylene Blends. *Ind. Eng. Chem. Res.* **2015**, *54*, 6108–6114.
- (6) Kalfoglou, N. K.; Skafidas, D. S.; Kallitsis, J. K.; Lambert, J.-C.; Van der Stappen, L. Comparison of compatibilizer effectiveness for PET/HDPE blends. *Polymer* **1995**, *36*, 4453–4462.
- (7) Zhang, H.; Zhang, Y.; Guo, W.; Xu, D.; Wu, C. Thermal properties and morphology of recycled poly(ethylene terephthalate)/maleic anhydride grafted linear low-density polyethylene blends. *J. Appl. Polym. Sci.* **2008**, *109*, 3546–3553.
- (8) Sharma, P.; Lochab, B.; Kumar, D.; Roy, P. K. Sustainable Bisbenzoxazines from Cardanol and PET-Derived Terephthalamides. *ACS Sustainable Chem. Eng.* **2016**, *4*, 1085–1093.
- (9) Fukushima, K.; Lecuyer, J. M.; Wei, D. S.; Horn, H. W.; Jones, G. O.; Al-Megren, H. A.; Alabdulrahman, A. M.; Alsewailem, F. D.; McNeil, M. A.; Rice, J. E.; Hedrick, J. L. Advanced chemical recycling of poly(ethylene terephthalate) through organocatalytic aminolysis. *Polym. Chem.* **2013**, *4*, 1610–1616.
- (10) Palekar, V. S.; Shah, R. V.; Shukla, S. R. Ionic liquid-catalyzed aminolysis of poly(ethylene terephthalate) waste. *J. Appl. Polym. Sci.* **2012**, *126*, 1174–1181.
- (11) Shah, R. V.; Shukla, S. R. Effective aminolytic depolymerization of poly(ethylene terephthalate) waste and synthesis of bisoxazoline therefrom. *J. Appl. Polym. Sci.* **2012**, *125*, 3666–3675.
- (12) Pillon, L. Z.; Utracki, L. A. Compatibilization of polyester/polyamide blends via catalytic ester-amide interchange reaction. *Polym. Eng. Sci.* **1984**, 24, 1300–1305.
- (13) Pillon, L. Z.; Utracki, L. A.; Pillon, D. W. Spectroscopic study of poly(ethylene terephthalate)/poly(amide-6,6) blends. *Polym. Eng. Sci.* **1987**, 27, 562–567.
- (14) Gug, J.; Sobkowicz, M. J. Improvement of the mechanical behavior of Bioplastic poly(lactic acid)/polyamide blends by reactive compatibilization. *J. Appl. Polym. Sci.* **2016**, *133*, 43350.
- (15) Wang, M.; Yuan, G.; Han, C. C. Influences of hyperbranched polyethylenimine on the reactive compatibilization of polycarbonate/polyamide blends. *Chin. J. Polym. Sci.* **2015**, *33*, 652–660.
- (16) Morita, T.; Maughon, B. R.; Bielawski, C. W.; Grubbs, R. H. A Ring-Opening Metathesis Polymerization (ROMP) Approach to Carboxyl- and Amino-Terminated Telechelic Poly(butadiene)s. *Macromolecules* **2000**, *33*, 6621–6623.
- (17) Ji, S.; Hoye, T. R.; Macosko, C. W. Diamino telechelic polybutadienes for solventless styrene-butadiene-styrene (SBS) triblock copolymer formation. *Polymer* **2008**, *49*, 5307–5313.
- (18) Martinez, H.; Ren, N.; Matta, M. E.; Hillmyer, M. A. Ring-opening metathesis polymerization of 8-membered cyclic olefins. *Polym. Chem.* **2014**, *5*, 3507–3532.
- (19) Nagarkar, A. A.; Crochet, A.; Fromm, K. M.; Kilbinger, A. F. M. Efficient Amine End-Functionalization of Living Ring-Opening Metathesis Polymers. *Macromolecules* **2012**, *45*, 4447–4453.
- (20) Feigenbaum, A.; Lehn, J. M. Kinetic and conformational studies by NMR. XX. Ring inversions of 4,9-dihetero-cis,cis-1,6-cyclodecadiene systems. *Bull. Soc. Chim. Fr.* **1973**, 198–202.
- (21) Moore, W. R.; Sanderson, D. Viscosities of Dilute Solutions of Polyethylene Terephthalate. *Polymer* **1968**, *9*, 153–158.
- (22) Wilson, G. O.; Porter, K. A.; Weissman, H.; White, S. R.; Sottos, N. R.; Moore, J. S. Stability of Second Generation Grubbs' Alkylidenes to Primary Amines: Formation of Novel Ruthenium-Amine Complexes. *Adv. Synth. Catal.* **2009**, *351*, 1817–1825.

(23) Rawal, V. H.; Cava, M. P. Thermolytic removal of t-butyloxycarbonyl (BOC) protecting group on indoles and pyrroles. *Tetrahedron Lett.* **1985**, *26*, 6141–6142.

- (24) Leonard, J. K.; Wei, Y.; Wagener, K. B. Synthesis and Thermal Characterization of Precision Poly(ethylene-co-vinyl Amine) Copolymers. *Macromolecules* **2012**, *45*, 671–680.
- (25) Kaiser, E.; Colescott, R. L.; Bossinger, C. D.; Cook, P. I. Color test for detection of free terminal amino groups in the solid-phase synthesis of peptides. *Anal. Biochem.* **1970**, *34*, 595–598.
- (26) Hoteling, A. J.; Mourey, T. H.; Owens, K. G. Importance of Solubility in the Sample Preparation of Poly(ethylene terephthalate) for MALDI TOFMS. *Anal. Chem.* **2005**, *77*, 750–753.
- (27) Pracella, M.; Rolla, L.; Chionna, D.; Galeski, A. Compatibilization and properties of poly(ethylene terephthalate)/polyethylene blends based on recycled materials. *Macromol. Chem. Phys.* **2002**, 203, 1473–1485.
- (28) Anderson, K. S.; Hillmyer, M. A. The influence of block copolymer microstructure on the toughness of compatibilized polylactide/polyethylene blends. *Polymer* **2004**, *45*, 8809–8823.
- (29) The mechanical properties of HDPE were measured using identical conditions to the blends. Values are averaged over three trials: $E=0.8\pm0.2$ GPa, $\sigma_{\rm YS}=23\pm1$ MPa, and $\varepsilon_{\rm b}=569\pm49\%$.